

Visual Field and Task Influence Illusory Figure Responses

Afiza Abu Bakar,^{1,2*} Lichan Liu,² Markus Conci,³ Mark A. Elliott,^{3,4}
and Andreas A. Ioannides^{1,2}

¹*Department of Brain Science and Engineering, Graduate School of Life Science and Systems Engineering, Kyushu Institute of Technology, Kyushu, Japan*

²*Laboratory for Human Brain Dynamics, RIKEN Brain Science Institute, Wakoshi, Japan*

³*Experimental Psychology, Department of Psychology, Ludwig-Maximilians University, Munich, Germany*

⁴*Department of Psychology, National University of Ireland, Galway, Republic of Ireland*

Abstract: In normal viewing conditions, many objects are often hidden or occluded by others, therefore restricting the information that enters the eye. One ability that the human visual system has developed to compensate for this visual limitation is to relate the surrounding elements to globally interpret the whole scene. The appearance of illusory figures (IF) based on surrounding elements also relies on this similar function. In the present study, we hypothesized that different mechanisms may be used by the brain to process IF from the center and periphery of the visual field. We compared magnetoencephalographic responses to IFs presented at different parts of the visual field under three task loads. For central presentation, IF specific responses peaked first in V1/V2 (96–101 ms), and then in the lateral occipital complex (LOC; 132–141 ms), independent of task. For peripheral presentation, the relative modulation towards IF was markedly reduced in V1/V2 and LOC while prominent activation peaks now shifted to the Fusiform Gyrus (from 200 ms onwards). Additionally, the type of task influenced processing at early stages beginning in V1/V2 (87 ms). Our results show that retinal eccentricity plays a crucial role in IF processing: figural completion at the center of the visual field is achieved in an ‘automatic’ and seemingly effortless fashion whereas peripheral stimulus locations necessitate higher-order object completion stages which rely more heavily on attentional demands. *Hum Brain Mapp* 29:1313–1326, 2008. © 2007 Wiley-Liss, Inc.

Key words: Kanizsa; magnetoencephalography; magnetic field tomography (MFT); V1; V2; lateral occipital complex (LOC); fusiform gyrus

INTRODUCTION

Normal vision is achieved effortlessly regardless of missing information in the physical attributes of the visual input itself. Easy recognition of a moving car, a happy face, or an occluded object in a complex scene is performed smoothly because of the brain’s ability to interpret even the most complicated inputs into meaningful percepts. Kanizsa illusory figures (IF) [Kanizsa, 1955, 1976] demonstrate the capability of the visual system to integrate

*Correspondence to: Afiza Abu Bakar, Laboratory for Human Brain Dynamics, RIKEN Brain Science Institute, 2-1 Hirosawa, Wako-shi, Saitama, Japan 351-0198. E-mail: afiza@brain.riken.jp

Received for publication 23 February 2007; Revised 14 July 2007; Accepted 16 July 2007

DOI: 10.1002/hbm.20464

Published online 19 October 2007 in Wiley InterScience (www.interscience.wiley.com).

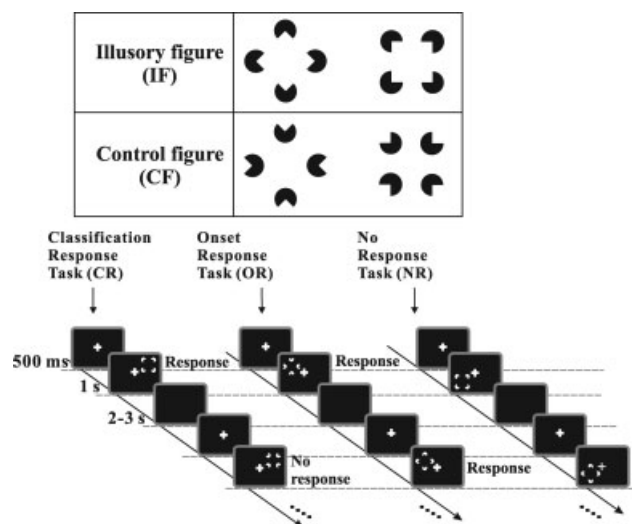


Figure 1.

The illusory figure (IF) and control (CF) figure stimuli used in the experiment are shown in the upper box. In IF, inducers were aligned to produce an illusory surface. The lower part of the figure shows examples of the experiment procedure for peripherally presented stimuli for each task condition. A fixation point appeared for 500 ms before a one-second stimulus presentation. Subjects were required to respond as soon as possible after the stimulus appeared on the screen. A black screen appeared on the screen for a randomized period of 2–3 sec after the stimulus presentation to indicate end of trial. Types of stimuli used and sequence in one run were the same for central conditions, except that stimuli appeared at the center of the screen. The stimuli here are not drawn to the same scale as the originally presented stimuli.

independent parts into a unitary representation in the absence of luminance- or chromatically- defined borders [see Fig. 1 (IF) for examples]. Although IF do not depict the boundaries defined by a physical border, a central, bright figure appears, defined by sharp, illusory contours projecting from aligned continuations with its surface appearing closer and overlapping the seemingly more distant inducer disks. Elucidating the functional mechanism that underlies the perception of IF may contribute to the understanding of how information is integrated along the visual system.

The focus of IF studies have expanded from identifying areas sensitive to IF processing towards understanding how information is shared between various brain areas along the process of its perception. In this study, we exploit the high temporal resolution of Magnetoencephalography (MEG) to study the mechanisms of IF processing separately for central and peripheral vision. Central and peripheral vision has been shown to hold functional bias towards complicated objects such as buildings and faces [Levy et al., 2001, 2004; Liu and Ioannides, 2006]. IF perception, which also requires complex processing, may

therefore employ different mechanisms for central and peripheral visual fields, as demonstrated in some behavioral observations [Atchley and Atchley, 1998; Rubin et al., 1996].

Earlier physiological studies have exhibited the ability of early visual areas such as V1 and V2 [Lee and Nguyen, 2001; Peterhans and von der Heydt, 1989; von der Heydt et al., 1984] to detect illusory contours. Some human behavioral studies have also suggested a key role of V1 in perceiving IFs [Maertens and Pollmann, 2007; Pillow and Rubin, 2002]. Positron emission tomography (PET) [Ffytche and Zeki, 1996] and fMRI [Hirsch et al., 1995] studies on the other hand, have shown robust responses towards IFs in V2. Although the involvement of early visual areas in IF processing is necessary, the role of higher visual areas with larger receptive fields cannot be discounted. One area that has always been found to associate with IF processing is the lateral occipital complex (LOC). This area, known to respond towards images of objects [Malach et al., 1995] and object fragments [Grill-Spector et al., 1998], is a good candidate to capture the global organization involved in the perception of an IF. In fact, most human imaging studies have identified activity enhancement in LOC in response to IFs [Halgren et al., 2003; Mendola et al., 1999; Murray et al., 2002a; Murray et al., 2004]. Traces of a network of activity in the occipitotemporal cortex in response to IFs can be observed from the previous results of physiological and imaging studies, mostly performed for the central visual field. A physiological study on monkeys showed that V1 and V2 responded to illusory contours in a top-down manner [Lee and Nguyen, 2001], presenting evidence that there exist a lateral or feedback connection at the earliest stages of processing. Neuroimaging studies have also revealed a network of activity in response to IFs. This network includes V1 and V2 [Ffytche and Zeki, 1996; Hirsch et al., 1995; Seghier and Vuilleumier, 2006], LOC, fusiform gyrus (FG), and parietal cortices [Halgren et al., 2003; Murray et al., 2002a; Stanley and Rubin, 2003]. While early responses in V1 and V2 have been implicated in computing the contour of an IF, activations in higher areas have been suggested as estimating the surface characteristics of the enclosed salient regions [Stanley and Rubin, 2003].

In the present study, we investigated the locus and the time course of activations in response to IFs at central and peripheral visual field locations. We have also varied tasks, to observe their effects on IF processing in the central and peripheral visual field. Behavioral results of the present study revealed that central stimulus presentations elicited faster responses than those presented at one of the four quadrants. Magnetic field tomography (MFT) [Ioannides et al., 1990; Taylor et al., 1999] was employed to investigate brain responses towards IFs in different tasks and visual field presentations. Our results suggest that the location where an IF is presented significantly influences the way in which it will be processed: Central presentations elicit an initial ‘automatic’ completion which is followed

subsequently by task related modulations. By contrast, presentations in the periphery require a higher amount of attentional resources. Task-specific modulations occurred at early stages of processing while responses related to figural extraction were shifted to the FG, presumably reflecting its higher-order role in object completion.

MATERIALS AND METHODS

Subjects

Seven male subjects participated in the MEG recordings (24–50 years, mean age 32.7 years). All of them were right-handed, with normal visual acuity and no neurological deficits. The experiment was approved by the RIKEN Ethical Committee according to the Helsinki Declaration of 2000. The procedures were described to participants before they gave their informed, written consent.

Stimuli

Four types of stimulus configurations were used: two of them were diamond- and square-shaped Kanizsa-type IFs while the other two were control figures (CFs). The CFs was constructed with “Pac-Man” elements rotated 180° such that no IF could be perceived (see Fig. 1). The stimuli were presented at one of five screen locations (center or quadrants), blocked for each run. Hereafter, we refer to the presentation locations as center middle (CM), upper left (UL), upper right (UR), lower left (LL), and lower right (LR). Because of the difference in cell density between the fovea and periphery at early stages of visual processing, visual acuity for stimuli at the center is better than those presented at the periphery [Curcio and Allen, 1990; Rovamo and Virsu, 1979]. For this experiment, we have used larger stimuli sizes for peripheral stimuli as compared with those presented at the center to compensate for the decrease of perception for complex stimuli in the peripheral visual field [Rovamo et al., 1997]. At CM, the stimuli subtended $4^\circ \times 4^\circ$ of visual angle, with each Pac-Man element 1.3° in diameter. In the periphery, the stimuli were $6^\circ \times 6^\circ$, with an eccentricity of 10° , with each Pac-Man element 2° in diameter. Stimuli were delivered via video projector placed outside the shielded room and presented to subjects on a back-projection screen at a viewing distance of ~ 57 cm. A photodiode was attached to the screen to detect the exact onset time of each stimulus.

Task

Figure 1 shows the temporal sequence of a trial: First, a fixation cross appeared on the screen for 500 ms, followed by the stimulus (four types, randomized within a run) presented at the predetermined location for 1 sec. Subjects fixated on the center of the screen and responded to the stimuli based on the task, as instructed before each run. There were three types of tasks in the experiment: First, a classi-

fication response (CR) task, in which subjects responded to illusory-diamonds or squares by lifting the left or right index finger (counterbalanced across subjects). No response was required for the CFs. Second, there was an “onset response” (OR) task in which subjects responded whenever a stimulus was shown. The OR task was used to monitor preparation prior to motor responses and attentional effects whenever a response was required. In both the CR and OR tasks, subjects were required to give their responses as soon as possible after the stimuli appeared on the screen. Finally, in the “no response” (NR) task, subjects viewed the stimuli passively. This task was used as a control to compare our results with previous studies where passive viewing of IF was employed. A trial ended with a black screen shown for 2–3 sec.

MEG Signal Recording

Forty runs were recorded for each subject: 20 runs for the CR task (four repetition runs for each of the five stimulus locations), 10 runs each for the OR and NR tasks (two repetition runs for each location). The location of presented stimuli was fixed for every run. The order of the task runs was counter-balanced across subjects. In each run, there were 32 trials, eight for each of the four stimulus types. Stimuli type was randomized throughout each run.

Before the MEG experiment, three head coils were attached to each subject’s nasion, and left and right pre-auricular points to record head position. Subject head movements remained within 4 mm for all runs. We recorded MEG signals using a whole-head Omega 151-channel system (CTF, Vancouver, Canada). Additional electrodes were placed to monitor subject artifacts such as vertical and horizontal eye movements. These consisted of EOG electrodes placed 1 cm lateral to the left and right outer canthus of the eyes for vertical movements, and 1 cm above and below the left eye for horizontal eye movements. Heartbeat was monitored via electrodes on the left and right arms, left foot, and on the back. During the recording, the MEG signal was low-pass filtered at 200 Hz, and sampled at 625 Hz, continuously for each run of about 3 min. The whole recording process lasted for about 2 h.

Co-Registration of MEG and MRI

For each subject, high-resolution anatomical, T1-weighted MRI images (voxel size, $1 \times 1 \times 1$ mm³) were collected with a 1.5-T Siemens MRI scanner. Each subject’s head shape was scanned using a 3D digitizer (Fastrak, Polhemus, Colchester, USA). Each digitized head shape was fitted to the MRI image to obtain a transformation matrix between coil- and MRI-based coordinate systems using dedicated in-house software [Hironaga et al., 2002]. The co-registration accuracy was manually checked and matched to within 1–2 mm.

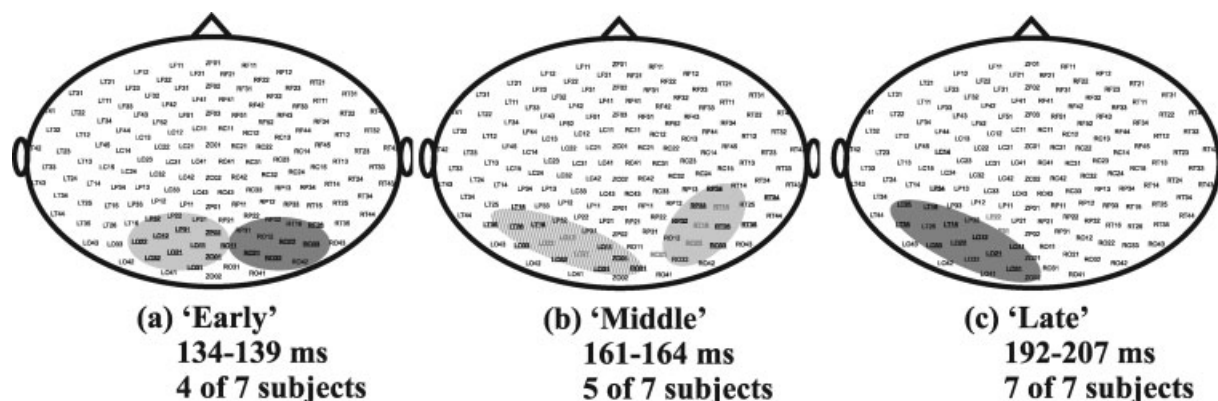


Figure 2.

Distribution of sensors with high SNR values, divided into early, middle, and late components. The numbers at the bottom of each figure indicate the mean latency of high SNR peaks, and number of subjects showing these responses over the total number of participants. The light grey surface indicates a tendency of peaks having negative values; dark grey is for positive values; and lined surfaces for peaks having no specific tendency towards either polarity.

MEG Signal Analysis

Signal processing

Off-line, environmental noise was first removed from the MEG signal by taking the third gradient of the magnetic field. The resulting data were filtered using the CTF software in the 1–200 Hz band with notch filters at 50 Hz and its harmonics to eliminate noise generated by the power line. Through careful off-line inspection, we rejected trials contaminated by eye movements close to stimulus onset (–250 to 900 ms), and responses before or during image onset, as well as double responses (i.e. when subjects lifted both left and right fingers). About three percent of the trials across subjects were discarded. For the remaining data, we extracted trials from each run, 200 ms before, to 850 ms after stimulus onset. We also removed subject artifacts such as cardiac rhythm and eye movements and blinks using independent component analysis (ICA) [Jahn et al., 1999]. In each run, the ICA-cleaned data were aligned on the stimulus onset and averaged according to stimulus type. There were eight trials in each averaged signal. If there were fewer than five trials available for averaging in a condition, this condition was excluded from further analyses.

Signal-to-noise ratio based selection

To identify “responsive sensors,” we performed a signal-to-noise ratio (SNR) analysis on the MEG signals from each sensor. If a sensor had a high SNR peak value, that sensor was considered to have higher signal content compared with the background noise, and thus to be more responsive to the presented stimulus. The SNR was defined

as the mean amplitude divided by its standard deviation in a 10-ms window. The center of the window was moved in 1.6-ms steps through the 0- to 300-ms interval after the stimulus onset.

The SNR analysis was conducted on runs when the stimuli were presented at the center in the following three steps: First, for each subject, 10 sensors with the highest SNR values were selected for each of the four stimulus types in each run. For these sensors, we further selected those with SNR values greater than 10 (but only 7 for one subject). This resulted in a list of the most responsive sensors for each subject. Second, we put all the selected sensors from each subject together and sorted the sensors into three groups based on their peak latencies: early (134–139 ms), middle (161–164 ms), and late (192–207 ms). Finally, overlapping channels across subjects in the three groups were obtained and mapped, as shown in Figure 2.

Distributed Source Analysis

We applied MFT, a distributed source method, to obtain millisecond-by-millisecond estimates of brain activity. MFT produces probabilistic estimates for the nonsilent primary current density vector $\mathbf{J}(\mathbf{r}, t)$ at each time-slice of the MEG signal [Ioannides et al., 1990]. The MFT algorithm relies on a nonlinear solution to the inverse problem, which has optimal stability and sensitivity for localized distributed sources [Taylor et al., 1999]. For each subject, four hemispheric source spaces were defined, each covering the left, right, superior, and posterior parts of the brain well. Lead fields used for the MFT analysis were computed from a spherical head model for the conductivity of the head, defined separately for each one of the four source spaces.

The center of the sphere was chosen by finding the best fit to the local curvature of the inner surface of the skull below a set of 90 MEG channels. MFT was used to extract brain activity separately from the signal corresponding to the 90 channels (closest to the source space) selected for each of the four source spaces. The results from the four source spaces were then combined into one large source space covering the entire brain and stored in an $8 \times 8 \times 8$ mm³ source space grid. The details of the method can be found elsewhere [Ioannides et al., 1990, 1995; Taylor et al., 1999]. For each subject, we applied MFT to the averaged data for each stimulus type in each run, from 100 ms before, to 400 ms after stimulus onset in 1.6 ms steps. The MFT analysis of the average signal gave estimates for the current density vector at each source space grid point and time-slice for each condition in each run of each subject.

Post-MFT Statistical Parametric Mapping Analysis

Since the MFT computation was performed independently for each time-slice, we were able to treat the modulus of the current-density vector at each time-slice and source space grid point as an independent random variable. We could therefore use statistical parametric mapping (SPM) to identify brain areas and latency periods when the activity was significantly different between conditions [Ioannides, 2001].

The SPM analysis used the moduli of the current density vector. For each grid point and at each time-slice, the unpaired *t*-test was used to test the null hypothesis (i.e. that the two distributions were the same). We used the conservative Bonferroni adjustment to correct for multiple grid-point comparisons. This statistical analysis makes no a priori assumptions about any regional activity or timing because it identifies loci of significant changes of activity in a model-independent manner, that is, grid point-by-point statistical analysis throughout the entire brain for each time-slice.

To identify brain activation related to the stimuli that was significantly different from the prestimulus baseline period, we compared the distribution at a given poststimulus latency with that in the prestimulus period, separately for each stimulus type in each run. Typically, the SPM maps for this contrast showed a rather brief focal activation that spread quickly over wide brain areas. We also directly compared two distributions from two conditions (e.g. IFs versus CFs of the same shape presented in the same part of the visual field and under the same task condition). In this comparison, the SPM maps were based on two distributions, for the same poststimulus latency, but corresponding to responses to two distinct conditions.

The SPM maps of individual subjects were then transformed to a common Talairach space [Talairach and Tournoux, 1988] so that common active brain areas across subjects could be identified. This procedure produced new maps that contained, in each source-space grid point and at each timeslice, the number of subjects that showed a

consistent change in activity at a predefined *P*-value. A positive number was used for increases and a negative number for decreases. These combined maps were then back-transformed to the MRI space of one subject for display purposes.

Regional Brain Activations

Definition for ROIs

The initial estimates for the locations of regions of interest (ROIs) were based on the consistent activations in the combined SPM maps across subjects. Four ROIs were evident for V1/V2, each defined for the different parts of the cortex activated by the stimulus at different locations (e.g. For the CM location, four V1/V2 ROIs were defined for the left/right/dorsal/ventral areas around the calcarine sulcus; for the UL, only one V1/V2 ROI was defined for the right ventral area). For LOC, two ROIs were defined in each hemisphere, to allow for activations in the dorsal and ventral regions along the middle occipital gyrus. Consistent activity was also seen in the FG, therefore one ROI for FG was selected in each hemisphere. These initial estimates were then transformed to the MRI coordinates of each subject and the ROIs were adjusted using the maxima of the MFT solutions, separately for each subject. The above procedure produced 20 ROIs for each subject, 10 from the central, and 10 from the peripheral presentations (see Table I). All ROIs were defined with a radius of 1 cm.

Direction of current density vector

Because the MFT solutions produce a current-density vector $\mathbf{J}(\mathbf{r}, t)$ without any radial component, the direction for $\mathbf{J}(\mathbf{r}, t)$ is essentially confined to two dimensions and its variation can be conveniently quantified and displayed using circular statistics [Fisher, 1993; Ioannides et al., 2005]. For each ROI, we obtained the “main direction” from the circular statistics which yielded a stable direction at time ranges corresponding to the earliest or peak activation in that ROI. In the present study, we selected the “main direction” from the CR task. For V1/V2 ROIs, we defined the direction using a latency range of 50–100 ms; and for the LOC and FG, we used a range of 100–150 ms. The strongest current-density distribution within these time ranges was selected as the main direction for each ROI.

Activation Time Courses and Statistical Analysis

For each condition in each run, we calculated an ROI activation time course (ACV) $J_1(t) = \int_{\text{ROI}} \mathbf{J}(\mathbf{r}, t) \cdot \hat{\mathbf{u}}_{\text{ROI}} d^3\mathbf{r}$ with $\hat{\mathbf{u}}_{\text{ROI}}$ defined as the main direction of the current-density vector. We further applied analysis of variance (ANOVA, SPSS, Chicago, IL) to the ACVs to examine whether ROI activation time-courses were significantly different between pairs of conditions.

TABLE I. List of Talairach coordinates for central and peripheral stimuli

		Central presentation	Peripheral presentation
V1/V2 ROIs ^a	Left Dorsal V1/V2	-8 ± 3, -94 ± 4, 3 ± 7	-9 ± 3, -86 ± 4, 4 ± 6
	Right Dorsal V1/V2	10 ± 5, -89 ± 3, 3 ± 3	9 ± 4, -85 ± 3, 5 ± 4
	Left Ventral V1/V2	-8 ± 2, -87 ± 4, -9 ± 7	-10 ± 3, -74 ± 7, -3 ± 3
	Right Ventral V1/V2	9 ± 4, -85 ± 4, -9 ± 5	7 ± 5, -79 ± 8, -4 ± 5
Extrastriate ROIs ^b	L-LOC Dorsal	-37 ± 6, -74 ± 8, 15 ± 7	-36 ± 4, -76 ± 7, 17 ± 5
	L-LOC Ventral	-37 ± 8, -77 ± 9, -6 ± 5	-36 ± 5, -77 ± 5, -6 ± 3
	R-LOC Dorsal	34 ± 5, -71 ± 7, 15 ± 4	35 ± 4, -71 ± 7, 13 ± 5
	R-LOC Ventral	37 ± 8, -73 ± 7, -4 ± 5	36 ± 4, -75 ± 5, -6 ± 3
	L-FG	-36 ± 6, -59 ± 9, -10 ± 4	-33 ± 5, -52 ± 6, -10 ± 3
	R-FG	32 ± 5, -56 ± 10, -9 ± 3	33 ± 6, -53 ± 9, -9 ± 3

^aTalairach coordinates x, y, z (mean ± SD) in mm for V1/V2 ROIs.

^bTalairach coordinates x, y, z (mean ± SD) in mm for extrastriate ROIs.

The ANOVA was performed separately for the central and peripheral presentations. Each ACV was computed from 100 ms before, to 380 ms after the stimulus onset, in 1.6 ms time-window steps. In the analysis, Subject was considered a random factor, and the following five factors were used as fixed factors when applicable: (1) Task (CR, OR, NR); (2) IF (present, absent); (3) Shape (square, diamond); (4) ROI hemisphere (left, right) and (5) ROI-position (dorsal, ventral). In this article, we report main effects at $P < 0.05$ and interactions at $P < 0.01$ when IF or task factors were used.

RESULTS

Behavioral Results

Reaction-time (RT) data were available for two of the three tasks, namely for the CR and OR task. No behavioral measure was available for the third NR task, as this aimed to provide task-independent MEG measures and only required the passive viewing of the stimulus. Measures of accuracy showed that subjects performed well, with correct responses ranging from 89 to 96% across subjects. For the purpose of RT analysis, erroneous responses were discarded from the data.

Analysis of RTs for the CR task showed that stimuli presented at the center were processed faster than stimuli presented at peripheral locations (mean response latencies: 626 ms and 642 ms, respectively). However, ANOVA analysis indicated that the effect did not achieve significance ($F_{(1,6)} = 2.8, P < 0.15$). An ANOVA performed on the response times across tasks showed that subjects responded on average 212 ms earlier in the OR task than in the CR task ($F_{(1,6)} = 31.7, P < 0.001$). No significant differences were found for shape or location.

SNR Analysis of MEG Signals

SNR analysis of the raw MEG signals identified strong and consistent brain responses to stimulus presentation in

posterior channels, indicating the involvement of striate and extrastriate visual cortex. The SNR analysis showed 3 time ranges characterized by strong consistent activity; an early (135 ± 6 ms; 4/7 subjects; see Fig. 2a), middle (163 ± 9 ms; 5/7 subjects; see Fig. 2b), and late (198 ± 16 ms; 7/7 subjects; see Fig. 2c) range, all from the posterior channels.

Activation Map Construction and ROI

Sources of brain activation were reconstructed at each time slice (1.6 ms) across the whole brain using MFT analysis [Ioannides et al., 1990], from the MEG signals after noise elimination (such as eye movements and incorrect trials). SPM analysis was then performed to obtain statistical maps between different experimental parameters. The experimental parameters were; task, shape, location, and condition (see Methods Section). Comparison of poststimulus with baseline periods showed activations at early latencies across subjects. Stimuli in this experiment are not ideal for V1 activation because of the limited surface area of the inducers, so although early activations in V1/V2 were seen in all cases, they did not reach significance for all visual field locations and task. The earliest response showing a statistically significant difference in V1/V2 was identified for CR central presentation at 47 ms.

SPM analysis between conditions (IF vs. CF) revealed enhancements of activity ($P < 0.05$) along the calcarine, middle occipital regions, and FG, indicating higher responses towards IFs. ROIs were placed at the identified regions for individual subjects for further analysis of their activation. An example SPM for central and peripheral stimulus locations and ROI of an individual subject is shown in Figure 3. The figure shows the SPMs for the IF versus CF contrast at $P < 0.05$ (yellow outlines). The blue circles show the ROIs for this subject (see Methods Section for description of the ROI definition). For this subject, the V1/V2 border was obtained in a separate experiment (shown in green outlines), so activations in V1 could be confirmed within these borders. Enhancement of activation towards IFs was found to be larger for central stimuli in

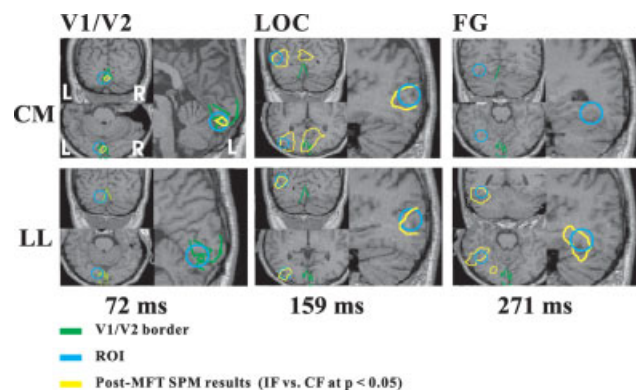


Figure 3.

Statistical analysis of MFT solutions showing significant modulation for IF as compared to CF for one subject, at three latencies. Each box depicts three views of the same ROI (in blue circles). The yellow outlines represent significant modulations at $P < 0.05$. The upper row gives activations from the central (CM) and the lower row, from the lower left (LL) presentations. Green lines near the calcarine represent the V1/V2 borders. The earliest differential activity is seen in V1/V2 at 72 ms only for central stimuli. Activity modulations in LOC were present for both the central and peripheral presentations. FG on the other hand, showed no significant IF modulation for CM and a late significant IF modulation for the LL condition.

V1/V2 and LOC, while the enhancement in FG was higher for peripheral presentation.

Activation Curve Statistical Analysis

Statistical analyses between IF and CF conditions were carried out to clarify their differences as a function of time. A time-course of activation was obtained from each ROI separately for each task, shape, location, and condition. Time-course of activations that were extracted from each individual subject showed that activities within each selected ROI were fairly stable across runs and conditions. An example of selected ROIs and their activation time-course at different runs and conditions taken from one subject is shown in Figure 4. Despite some variability in the response from run to run (clearly seen in Fig. 4b) the relative strength between IF and CF is maintained across runs. The average time-course of activation across subjects for task and condition were then compared for each ROI. Figure 5 shows activation curves from each ROI during central and peripheral presentation, averaged across all seven subjects. The top set of panels (a and b) show differences between stimulus conditions (IF vs. CF), and the bottom set (c and d) shows differences between tasks (CR vs. OR vs. NR). The first row of each set gives differences for centrally presented stimuli, while the second row gives differences for peripherally presented stimuli. Each curve

represents an average activation across subjects from one condition or task (Each defined by the colored bars within each box). Generally, activations in all three areas were lower for peripheral than centrally presented stimuli. Peaks of average activations were similar for central and peripheral locations, where V1/V2 activation peaked at around 100 ms, while LOC and FG peaked about 50 ms later. Activity for IF and CF conditions (red and blue curves) were almost identical in V1/V2 for both the central and peripheral presentations. For centrally presented stimuli, IFs were found to produce higher activations than CFs in LOC and FG. Peripheral presentation on the other hand, elicited amplitude modulation towards IFs in FG (Fig. 5b).

Task modulations (orange, green, and black curves) were elicited at different strengths in LOC and FG for centrally presented stimuli. This difference is prominent around the peaks of activations (around 150 ms) for both areas. When stimulus position is shifted to the periphery, a small difference in peak amplitude of activation between tasks can be observed in all areas, indicating some kind of discrimination between the three tasks at all stages of the visual system.

The latency and strength of differences between conditions and tasks were tested in each area for separate time slices (1.6 ms) by statistical analysis. Direct ANOVA comparisons between conditions revealed significant amplitude enhancements for IF- as compared with CF-configurations (what we term the “IF-effect”). However, the latencies and loci of activations differed markedly between central and peripheral locations. In addition, task demands (CR, OR, or NR) varied by central or peripheral presentation, revealing that brain activity accompanying the different tasks varied as a function of stimulus eccentricity. Table II summarizes statistically significant differences for central and peripheral presentations (Tables II). Figure 6 illustrates a summary of latencies of significant main effects for IF and Task.

For centrally presented stimuli and irrespective of task, an IF-effect was obtained at early stages of processing (96–101 ms) in V1/V2, (see Table II for details): specifically, IF stimuli elicited higher amplitudes than corresponding CF stimuli. The independence of this effect of task, suggests an early and automatic visual-cortical response to IFs. In addition, there was also an interaction effect between IF and shape (133–138 ms), where the amplitude difference between IF and CF configurations was larger for diamond as compared with square configurations.

In LOC, an IF-effect was observed at 128–176 ms, with the largest difference between IF and CF activation found at 132–141 ms ($P < 0.01$). Following this, a second enhancement of IF relative to CF occurred at 173–176 ms. Significant differences between tasks were also observed in LOC. From 141 to 158 ms CR and OR tasks produced higher amplitude than NR. At 271–277 ms (272–276 ms at $P < 0.01$), CR produced higher amplitudes than OR and NR tasks. Dorsal and ventral LOC showed an asymmetry in their activation (what we term the vertical-effect), i.e.,

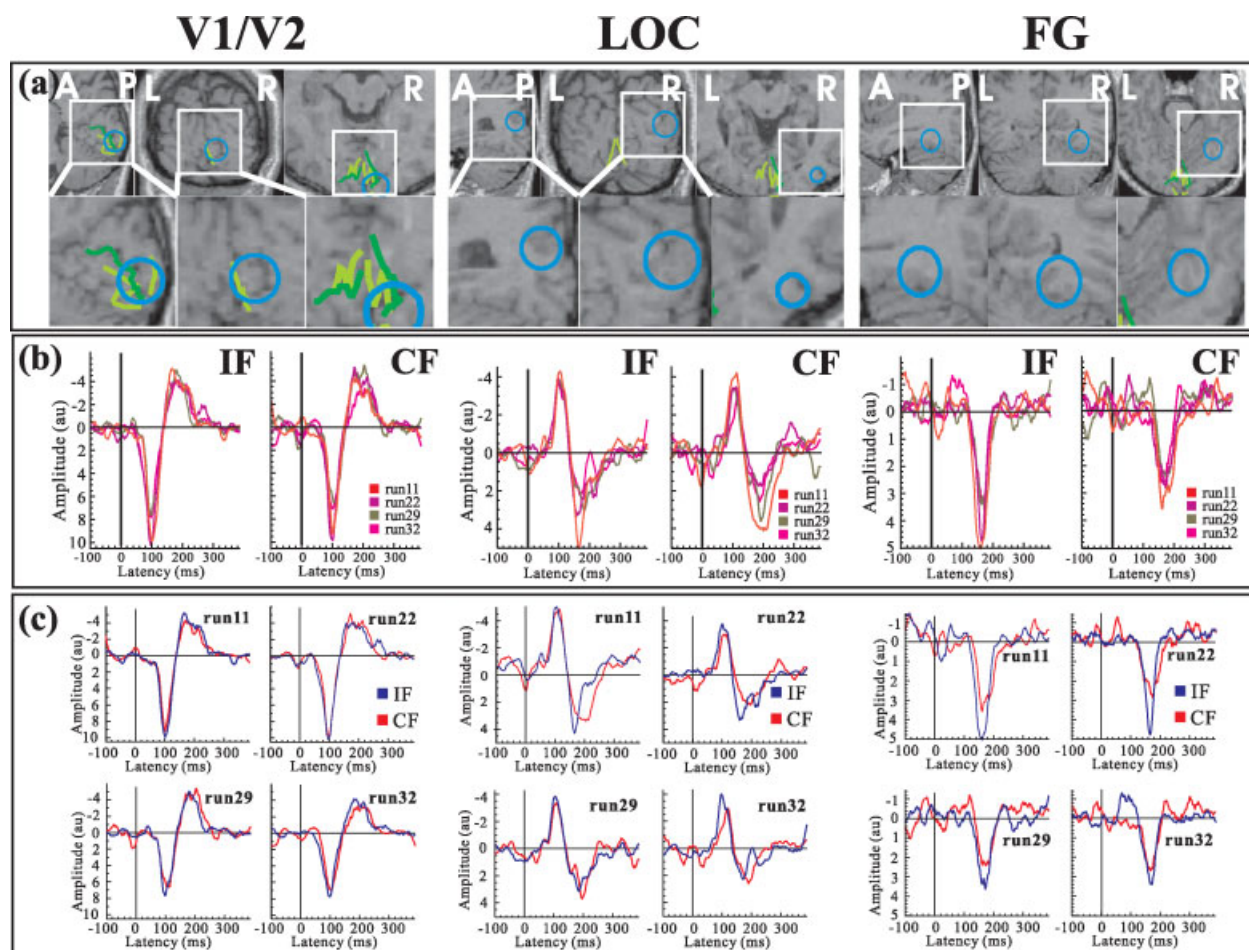


Figure 4.

An example of ROIs and their activation curves for one subject for a stimulus presented in the lower left quadrant of the visual field. The figure shows in three columns the results for three main areas in the right hemisphere (the hemisphere on the contralateral side of the stimulus presentation): Right dorsal V1/V2 ROI on the left column, the right dorsal LOC on the middle column and the right FG on the right column. (a) The loci of the ROIs are displayed in wide (top row) and zoomed (second row)

views. The blue circles represent the ROIs, the dark green outlines indicate the calcarine sulci, and the light green lines show the V1/V2 border as defined in a separate fMRI experiment. (b) the activation curves for each run are superimposed for different runs, but separately for IF and CF. (c) the activation curves for IF and CF are superimposed on the same figure, but separately for each run.

dorsal LOC elicited significantly higher responses than ventral LOC at 232–274 ms, irrespective of IF presence.

Unlike V1/V2 and LOC, the FG showed no IF-effect. Instead, a strong difference between CR and OR/NR tasks was found at 237–290 ms (247–276 ms and 279–287 ms at $P < 0.01$).

In summary, IFs presented at the center of the visual field are processed rapidly in early visual areas, producing IF-effects in V1/V2 at around 100 ms and at around 120–170 ms in LOC. At slightly delayed latencies, higher activations for CR and OR (as compared with NR), task demands suggest the influence of attentional deployment

(and possibly also motor response preparation) on LOC activations. Following this, the influence of task is again found in FG over a sustained period between 237 and 290 ms. Figure 6 (top panel) illustrates the timing of significant main effects of IF and task difference for centrally presented stimuli.

For peripheral stimulus presentations a different picture emerged. Significant task- and IF- effects were also observed, but these were identified at different latencies and activation loci from those found following central presentations. In general, activation differences between tasks were identified early and IF-effects late. In V1/V2 activa-

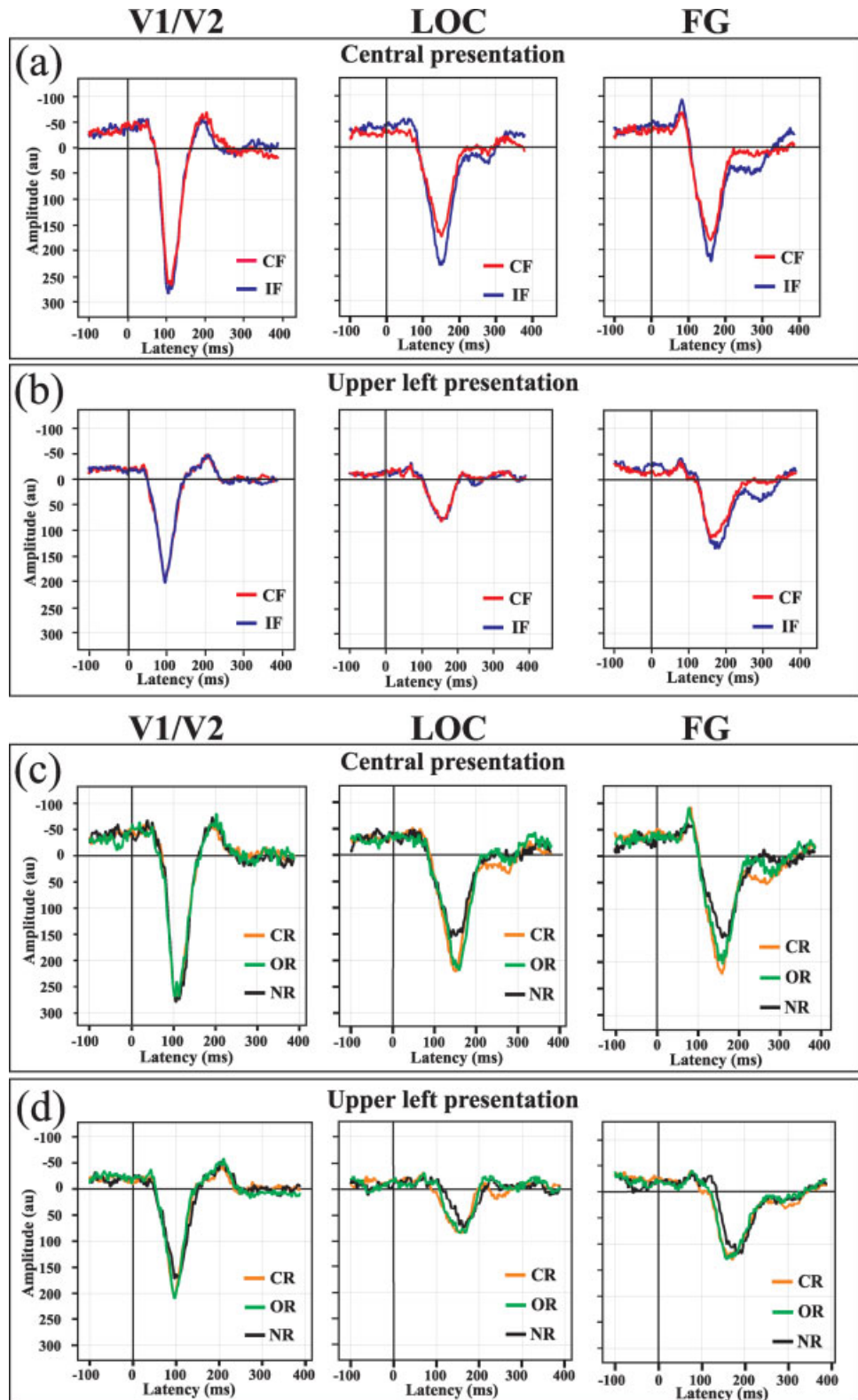


Figure 5.

Time course of activations across stimulus types and tasks for each ROI during central and peripheral conditions. Each curve represents an average activation from one task or condition (indicated in different colors), taken across all seven subjects. The upper rows show activations for IF and CF during central presentation (a) and upper left presentation (b). Activations across tasks are shown in the lower rows for central (c) and peripheral (d) stimuli.

TABLE II. Overview of statistically significant differences of ROI activation curves in areas V1/V2, LOC, and FG for centrally and peripherally presented stimuli

	ROI	Stimulus position	Effect	Latency range (ms)	Peak significant level		
Centrally presented stimuli ^a	V1/V2	All periphery conditions	IF	96.8–101.6	$F_{(1,6)} = 12.2$		
			IF × shape	133.6–138.4	$F_{(1,6)} = 22.0^*$		
	LOC		IF	128.8–164.0	$F_{(1,6)} = 18.1$		
			Task	132.0–141.6	$F_{(1,6)} = 13.8^*$		
	FG		Task	141.6–159.2	$F_{(2,12)} = 8.4$		
			ROI position	271.2–277.6	$F_{(2,12)} = 8.3$		
				272.8–276.0	$F_{(2,12)} = 8.3^*$		
			Task	232.8–274.4	$F_{(1,6)} = 86.4$		
				237.6–290.4	$F_{(2,12)} = 40.2$		
				247.2–276.0	$F_{(2,12)} = 14.3^*$		
279.2–287.2	$F_{(2,12)} = 15.3^*$						
Peripherally presented stimuli ^b	V1/V2	All periphery conditions	Task	79.2–95.2	$F_{(2,12)} = 18.5$		
	LOC		LL	Task	85.6–88.8	$F_{(2,12)} = 18.4^*$	
				IF	160.8–165.6	$F_{(1,6)} = 16.4$	
	UL		Task	130.4–144.8	$F_{(2,12)} = 11.4$		
				138.4–144.8	$F_{(2,12)} = 11.4^*$		
				87.2–104.8	$F_{(2,12)} = 10.3$		
				117.6–124.0	$F_{(2,12)} = 6.3$		
	FG		LL	Task	141.6–146.4	$F_{(2,12)} = 5.9$	
					168.8–178.4	$F_{(2,12)} = 7.7$	
					288.8–319.2	$F_{(2,12)} = 9.8$	
					300.0–303.2	$F_{(2,12)} = 8.8^*$	
					356.0–360.8	$F_{(2,12)} = 13.0$	
					292.0–298.4	$F_{(1,6)} = 11.5$	
			UL	IF	301.6–317.6	$F_{(1,6)} = 22.9$	
					268.0–314.4	$F_{(1,6)} = 36.7$	
					280.8–284.0	$F_{(1,6)} = 21^*$	
					288.8–292.0	$F_{(1,6)} = 32.4^*$	
					Task	112.8–122.4	$F_{(2,12)} = 10.4$
					114.4–119.2	$F_{(6,2)} = 10.4^*$	
	LR		Task	127.2–140.0	$F_{(2,12)} = 8.7$		
				143.2–148.0	$F_{(2,12)} = 5.1$		
				156.0–160.8	$F_{(2,12)} = 14.9^*$		
				156.0–167.2	$F_{(2,12)} = 14.8$		
				172.0–178.0	$F_{(2,12)} = 7.6$		
				266.4–290.4	$F_{(1,6)} = 30.3$		
				UR	IF	135.2–143.2	$F_{(1,6)} = 37.8$
						216.8–247.2	$F_{(1,6)} = 50.5$
						223.2–236.0	$F_{(1,6)} = 50.6^*$
319.2–336.8		$F_{(1,6)} = 34.8$					
Task	Task	330.4–335.2	$F_{(1,6)} = 26.6^*$				
		119.2–122.4	$F_{(2,12)} = 5.5$				
		133.6–136.8	$F_{(2,12)} = 5.0$				
		140.0–164.0	$F_{(2,12)} = 12.9$				
UR	Task	143.2–152.8	$F_{(2,12)} = 10.6^*$				
		157.6–162.4	$F_{(2,12)} = 12.9^*$				

^aSignificant effects (at $P < 0.05$; $*P < 0.01$) and F values for centrally presented stimuli

^bSignificant effects (at $P < 0.05$; $*P < 0.01$) and F values for peripherally presented stimuli (LL: Lower Left; LR: Lower Right; UL: Upper Left; UR: Upper Right).

tions task differences were seen at 79–95 ms (85–88 at $P < 0.01$), with higher responses for CR and OR relative to the NR task.

LOC activations exhibited similar differences, for stimulus presentations in the left visual field (LL and UL). For UL presentation, activations were larger for CR and OR relative to NR tasks from 87 to 124 ms. In contrast a later difference at 141–146 ms was due to increased CR activations relative to those found under OR and NR conditions.

For LL presentations, an identical difference between tasks emerged slightly later at 130–144 ms (138–144 ms at $P < 0.01$). In contrast to central presentations, a difference between IF and CF configurations was not found except for a relatively late but brief difference in activation observed at 160–165 ms following LL stimulus presentation. Clear evidence showing specificity of the dorsal or ventral LOC towards peripherally presented IFs was not found in this analysis.

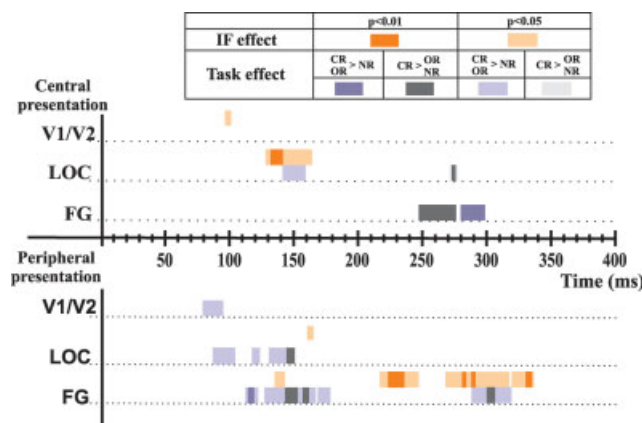


Figure 6.

The time course of significant activity for IF- and task effects across all subjects, for the central and peripherally presented stimulus conditions. The horizontal axis represents time, and the vertical axis separates brain areas. High contrast colors represent highly significant effects ($P < 0.01$) while low contrast colors represent lower significant effects ($P < 0.05$). Orange bars indicate the IF effect. Purple bars indicate task effects related to subjects' responses towards the stimuli (CR and OR > NR), while grey bars indicate task effects related to the processing of IFs (CR > OR and NR). Significant effects from each quadrant of the visual fields for peripheral conditions were collapsed onto the same activation axis, therefore the display for peripheral presentation is marked for latencies with a significant effect in at least one of four visual field quadrants.

FG activations showed large differences between tasks from 112 to 178 ms across all quadrants of the visual field. This was due to increased amplitudes for CR and OR tasks relative to the NR task (see Table II for corresponding ranges at $P < 0.01$). In addition, the CR task differed significantly from OR and NR tasks at 140–164 ms and 157–162 ms for the UR, and 156–160 ms for the LR quadrants. A later influence of task was observed for stimulus configurations presented in the LL visual field from 288–319 ms, with CR task differing significantly from OR and NR tasks from 300–303 ms. For FG, clear differences between IF and CF stimuli were found, from 216–317 ms for all presentation quadrants (see Table II for corresponding ranges at $P < 0.01$). Apart from these late modulations of IF activations, earlier IF differences were observable between 135 and 143 ms only for the upper right visual field.

To summarize, IFs presented in the periphery of the visual field result in different sequences of cortical activation as compared with centrally presented IFs. For central presentations, the IF is processed first in V1/V2 and LOC with task-dependent differences in activity emerging only later. In contrast, for peripheral stimulus presentations, task effects were detected early across all

areas studied (V1/V2; from 78 ms onwards; LOC, from 87 ms onwards; FG, from 112 ms onwards). Sustained IF effects were observed late, and only in FG (216–317 ms). Figure 6 (bottom panel) illustrates the corresponding time course of activations for peripheral stimulus presentations.

DISCUSSION

The results of the present study suggest that upon perceiving IFs, the brain uses two different mechanisms for the central and peripherally presented stimuli, where task requirements strongly affect the organization of each mechanism. Task demands did not appear to affect the early stages of IF processing for centrally presented stimuli, but preceded IF processing when stimuli were presented in the periphery of the visual field.

IF Effect

Central presentation

Previous electrophysiological and human studies have shown implications of both V1 and V2 towards illusory contour processing [Ffytche and Zeki, 1996; Lee and Nguyen, 2001; Peterhans and von der Heydt, 1989; von der Heydt et al., 1984]. For the central presentation, we found an early modulation of V1/V2 activity towards IF (from 80 ms). The early IF effect that was present in the early visual areas may result from the feedback signal projected back to V1 from higher areas. Activation of V1 neurons with similar tuning properties [Gilbert and Wiesel, 1989] follow lateral connections between neurons within V1 and feedback from lateral connections in higher visual areas [Angelucci and Bressloff, 2006], resulting in modulated activation for IFs when inducer elements are aligned. Although not consistently established in human imaging studies, evidence from the animal physiological work of Lee and Nguyen [2001] indeed suggests that there exist feedback of signals from neurons in V2 towards V1 in illusory contour processing. Human behavioral studies by Pillow and Rubin [2002], and Maertens and Pollmann [2007] have also demonstrated the necessity of V1 in building illusory contours based on their observations of decreasing behavioral responses resulting from impairment of V1. Consistent with our earlier studies [Moradi et al., 2003; Poghosyan et al., 2005], we found V1 activation much earlier, beginning at around 40 ms (data not shown), with early activations almost identical for both IF and CF stimuli. The V1/V2 IF modulation at 80 ms is sufficiently late to be explained by feedback interactions after the initial bottom-up driven pass of visual information through V1.

The activation of LOC which peaks at ~120–170 ms agrees with findings of IF-activation reported in other studies in terms of timing and location [Conci et al., 2006; Halgren et al., 2003; Murray et al., 2002a; Stanley and Rubin, 2003]. It is also consistent with the idea that LOC

mediates a generalized object-selective response preference [Grill-Spector et al., 1998; Kourtzi and Kanwisher, 2000; Lerner et al., 2002; Malach et al., 1995]. As an intermediate area within the visual system, LOC holds receptive fields large enough to be able to receive input from large regions of the visual field, consisting of information from a large number of interacting V1 and V2 neurons. The large amount of input from lower visual areas therefore allows LOC to perform global integration, which is also essential to IF perception. Also shown in a previous fMRI study by Stanley and Rubin [2003], is a role of LOC not in constructing the illusory contours per se, but rather in detecting salient organization of the whole figure, supporting the role of LOC as a global integrator of lower visual inputs.

Peripheral presentation

Peripherally presented IFs on the other hand, are processed using a different mechanism. The early IF effect in V1/V2 found for centrally presented stimuli was not seen for peripherally presented IFs. This is consistent with the insufficient feedback and callosal connections between neurons that code peripheral inputs [Kennedy et al., 1986], therefore limiting the sharp information that may exist based on illusory contour formation in early visual areas. The lack of this sharp information is likely to limit differences between IF and CF in the periphery at earlier stages of processing.

While the IF effect was all but eliminated in V1/V2, and greatly reduced in the LOC, it was robust in FG at later stages of processing (after 200 ms). With limited lateral connections, early visual areas are not able to properly propagate information despite feedback from higher areas. The higher visual areas on the other hand, are able to capture the global organization of the stimuli from feed-forward and feedback information obtained from earlier visual areas. Thus, when processing IFs in the periphery, the visual system shifts its processing locus towards the FG, which is at a higher position in the visual hierarchy and more sensitive to the global features of the perceived image [Lerner et al., 2001]. The prominent shift of activity to FG for peripheral IF presentations suggests that this area known to respond to many types of visual stimuli such as faces [Kanwisher et al., 1997] and other objects [Grill-Spector et al., 2006], is also responsive to IFs. IF differences in LOC and FG always coincided with relatively smaller activation differences in their corresponding lower-tier areas. For instance, central stimulus presentation resulted in maximal activation differences in LOC, but relatively smaller effects for V1 and V2 (see Fig. 5). Similarly, for peripheral presentations, FG was identified as the major source of differential activity, whereas for LOC and V1/V2 no comparable IF effect could be identified (see Fig. 5). This processing hierarchy could relate to suggestions that activations at early visual areas are reduced through feedback connections when shape

completion is achieved in higher visual areas [Murray et al., 2002b].

Task Effects

Overall, task effects were observed earlier during peripheral relative to central presentations (see Fig. 6, purple and grey bars). A closer look at these effects reveals that differences related to enhanced attention during manual response (that is, differences between CR and OR tasks relative to the NR task) were generally observed at shorter latencies (~80 ms earlier) than those related to the identification of a specific stimulus type (i.e., differences between the CR task relative to OR and NR tasks). This difference in the neural response between tasks corresponds to behavioral differences in response latencies (of 212 ms) and is consistent with previous studies showing constant delays between simple detection and stimulus identification tasks [Sagi and Julesz, 1984, 1985]. In addition, for central presentations, task effects were observed after processes attributed to IF completion in LOC (from 141 ms onwards), and FG (from 237 ms onwards). For peripheral presentations, task effects were present at all levels of cortical processing from 79 ms onwards in V1/V2, LOC and FG. This may indicate that peripheral presentations are modulated by task-related attentional demands earlier than central stimuli. It has been shown that task instructions can modulate the processing of early visual areas, also depicting variations of task-related activity-modulations with stimulus eccentricity [Jack et al., 2006]. Consistent with the study by Jack et al. [2006], the influence of task demands led to greater (and earlier) activity modulations when more peripheral retinal positions were engaged.

In summary, our results suggest that eccentricity plays a crucial role in determining how IFs are processed: completion of centrally located figural elements is achieved in an 'automatic' fashion, whereas peripheral stimulus locations necessitate higher-order figural completion mechanisms and are more sensitive to task, suggesting that these processes are highly susceptible to attentional control. The present study therefore provides us with new insights about how similar perceptual properties of the visual input are processed by two different mechanisms in the brain, depending on their position and the required task.

ACKNOWLEDGMENTS

We thank Dr. Hironaga for technical support during the experiments, Dr. Maruyama for advice on SPSS statistical procedures, Dr. Palomo for redaction of the manuscript and Dr. Poghosyan for helpful comments.

REFERENCES

- Angelucci A, Bressloff PC (2006): Contribution of feedforward, lateral and feedback connections to the classical receptive field center and extra-classical receptive field surround of primate V1 neurons. *Prog Brain Res* 154:93–120.

- Atchley RA, Atchley P (1998): Hemispheric specialization in the detection of subjective objects. *Neuropsychologia* 36:1373–1386.
- Conci M, Gramann K, Muller HJ, Elliott MA (2006): Electrophysiological correlates of similarity-based interference during detection of visual forms. *J Cogn Neurosci* 18:880–888.
- Curcio CA, Allen KA (1990): Topography of ganglion cells in human retina. *J Comp Neurol* 300:5–25.
- Ffytche DH, Zeki S (1996): Brain activity related to the perception of illusory contours. *Neuroimage* 3:104–108.
- Fisher NI (1993): *Statistical Analysis of Circular Data*. New York: Cambridge University Press.
- Gilbert CD, Wiesel TN (1989): Columnar specificity of intrinsic horizontal and corticocortical connections in cat visual cortex. *J Neurosci* 9:2432–2442.
- Grill-Spector K, Kushnir T, Hendler T, Edelman S, Itzhak Y, Malach R (1998): A sequence of object-processing stages revealed by fMRI in the human occipital lobe. *Hum Brain Mapp* 6:316–328.
- Grill-Spector K, Sayres R, Ress D (2006): High-resolution imaging reveals highly selective nonface clusters in the fusiform face area. *Nat Neurosci* 9:1177–1185.
- Halgren E, Mendola J, Chong CD, Dale AM (2003): Cortical activation to illusory shapes as measured with magnetoencephalography. *Neuroimage* 18:1001–1009.
- Hironaga N, Schellens M, Ioannides AA (2002): Accurate co-registration for MEG reconstructions. In: *Proceedings of the 13th International Conference on Biomagnetism*. VDE Verlag, Berlin. pp 931–933.
- Hirsch J, DeLaPaz RL, Relkin NR, Victor J, Kim K, Li T, Borden P, Rubin N, Shapley R (1995): Illusory contours activate specific regions in human visual cortex: Evidence from functional magnetic resonance imaging. *Proc Natl Acad Sci USA* 92:6469–6473.
- Ioannides AA (2001): Real time human brain function: Observations and inferences from single trial analysis of magnetoencephalographic signals. *Clin Electroencephalogr* 32:98–111.
- Ioannides AA, Bolton JP, Clarke CJS (1990): Continuous probabilistic solutions to the biomagnetic inverse problem. *Inverse Probl* 6:523–542.
- Ioannides AA, Liu MJ, Liu LC, Bamidis PD, Hellstrand E, Stephan KM (1995): Magnetic field tomography of cortical and deep processes: Examples of “real-time mapping” of averaged and single trial MEG signals. *Int J Psychophysiol* 20:161–175.
- Ioannides AA, Fenwick PB, Liu L (2005): Widely distributed magnetoencephalography spikes related to the planning and execution of human saccades. *J Neurosci* 25:7950–7967.
- Jack AI, Shulman GL, Snyder AZ, McAvoy M, Corbetta M (2006): Separate modulations of human V1 associated with spatial attention and task structure. *Neuron* 51:135–147.
- Jahn O, Chichocki A, Ioannides AA, Amari S (1999): Identification and elimination of artifacts from MEG signals using extended independent component analysis. In: Yoshimoto M, Kotani M, Kuriki S, Karibe H, Nakasato N, editors. *Recent Advances in Biomagnetism*. Sendai: Tohoku University Press. pp 224–228.
- Kanizsa G (1955): Margini quasi-percettivi in campi con stimolazione omogenea. *Rivista di Psicologia* 49:7–30.
- Kanizsa G (1976): Subjective contours. *Sci Am* 234:48–52.
- Kanwisher N, McDermott J, Chun MM (1997): The fusiform face area: A module in human extrastriate cortex specialized for face perception. *J Neurosci* 17:4302–4311.
- Kennedy H, Dehay C, Bullier J (1986): Organization of the callosal connections of visual areas V1 and V2 in the macaque monkey. *J Comp Neurol* 247:398–415.
- Kourtzi Z, Kanwisher N (2000): Cortical regions involved in perceiving object shape. *J Neurosci* 20:3310–3318.
- Lee TS, Nguyen M (2001): Dynamics of subjective contour formation in the early visual cortex. *Proc Natl Acad Sci USA* 98:1907–1911.
- Lerner Y, Hendler T, Ben Bashat D, Harel M, Malach R (2001): A hierarchical axis of object processing stages in the human visual cortex. *Cereb Cortex* 11:287–297.
- Lerner Y, Hendler T, Malach R (2002): Object-completion effects in the human lateral occipital complex. *Cereb Cortex* 12:163–177.
- Levy I, Hasson U, Avidan G, Hendler T, Malach R (2001): Center-periphery organization of human object areas. *Nat Neurosci* 4:533–539.
- Levy I, Hasson U, Harel M, Malach R (2004): Functional analysis of the periphery effect in human building related areas. *Hum Brain Mapp* 22:15–26.
- Liu L, Ioannides AA (2006): Spatiotemporal dynamics and connectivity pattern differences between centrally and peripherally presented faces. *Neuroimage* 31:1726–1740.
- Maertens M, Pollmann S (2007): Illusory contours do not pass through the “Blind Spot.” *J Cogn Neurosci* 19:91–101.
- Malach R, Reppas JB, Benson RR, Kwong KK, Jiang H, Kennedy WA, Ledden PJ, Brady TJ, Rosen BR, Tootell RB (1995): Object-related activity revealed by functional magnetic resonance imaging in human occipital cortex. *Proc Natl Acad Sci USA* 92:8135–8139.
- Mendola JD, Dale AM, Fischl B, Liu AK, Tootell RB (1999): The representation of illusory and real contours in human cortical visual areas revealed by functional magnetic resonance imaging. *J Neurosci* 19:8560–8572.
- Moradi F, Liu LC, Cheng K, Waggoner RA, Tanaka K, Ioannides AA (2003): Consistent and precise localization of brain activity in human primary visual cortex by MEG and fMRI. *Neuroimage* 18:595–609.
- Murray MM, Wylie GR, Higgins BA, Javitt DC, Schroeder CE, Foxe JJ (2002a): The spatiotemporal dynamics of illusory contour processing: combined high-density electrical mapping, source analysis, and functional magnetic resonance imaging. *J Neurosci* 22:5055–5073.
- Murray SO, Kersten D, Olshausen BA, Schrater P, Woods DL (2002b): Shape perception reduces activity in human primary visual cortex. *Proc Natl Acad Sci USA* 99:15164–15169.
- Murray MM, Foxe DM, Javitt DC, Foxe JJ (2004): Setting boundaries: brain dynamics of modal and amodal illusory shape completion in humans. *J Neurosci* 24:6898–6903.
- Peterhans E, von der Heydt R (1989): Mechanisms of contour perception in monkey visual cortex. II. Contours bridging gaps. *J Neurosci* 9:1749–1763.
- Pillow J, Rubin N (2002): Perceptual completion across the vertical meridian and the role of early visual cortex. *Neuron* 33:805–813.
- Poghosyan V, Shibata T, Ioannides AA (2005): Effects of attention and arousal on early responses in striate cortex. *Eur J Neurosci* 22:225–234.
- Rovamo J, Virsu V (1979): An estimation and application of the human cortical magnification factor. *Exp Brain Res* 37:495–510.
- Rovamo J, Makela P, Nasanen R, Whitaker D (1997): Detection of geometric image distortions at various eccentricities. *Invest Ophthalmol Vis Sci* 38:1029–1039.

- Rubin N, Nakayama K, Shapley R (1996): Enhanced perception of illusory contours in the lower versus upper visual hemifields. *Science* 271:651–653.
- Sagi D, Julesz B (1984): Detection versus discrimination of visual orientation. *Perception* 13:619–628.
- Sagi D, Julesz B. (1985): “Where” and “what” in vision. *Science* 228:1217–1219.
- Seghier ML, Vuilleumier P (2006): Functional neuroimaging findings on the human perception of illusory contours. *Neurosci Biobehav Rev* 30:595–612.
- Stanley DA, Rubin N (2003): fMRI activation in response to illusory contours and salient regions in the human lateral occipital complex. *Neuron* 37:323–331.
- Talairach J, Tournoux P (1988): *Co-Planar Stereotaxic Atlas of the Human Brain*. New York: Thieme Medical Publishers.
- Taylor JG, Ioannides AA, Muller-Gartner HW (1999): Mathematical analysis of lead field expansions. *IEEE Trans Med Imaging* 18:151–163.
- von der Heydt R, Peterhans E, Baumgartner G (1984): Illusory contours and cortical neuron responses. *Science* 224:1260–1262.